Vibration and Shock Testing of a 50 mm Aperture Unimorph Deformable Mirror

Sinje Leitz[a,d], Maximilian Gerhards[a], Sven Verpoort[a], Ulrich Wittrock[a], Maximilian Freudling[b], Andreas Grzesik[b], Markus Erhard[b], and Pascal Hallibert[c]

[a]Münster University of Applied Sciences, Stegerwaldstr. 39, 48565 Steinfurt, Germany
[b]OHB System AG, Manfred-Fuchs-Str. 1, 82234 Weßling, Germany
[c]European Space Agency, ESTEC, 2201 AZ Noordwijk, The Netherlands
[d]leitz@fh-muenster.de

ABSTRACT

We present our latest results on a refined unimorph deformable mirror which was developed in the frame of the ESA GSTP activity "Enabling Technologies for Piezo-Based Deformable Mirrors in Active Optics Correction Chains". The identified baseline concept with the soft piezoceramic material PIC151 successfully sustained all vibration requirements (17.8 gRMS random and 20 g sine) and shock testing (300 g SRS). We cover the mirror design development which reduces the stress in the brittle piezo-ceramic by 90 % compared to the design from a former GSTP activity. We briefly address the optical characterization of the deformable mirror, namely the achieved Zernike amplitudes as well as the unpowered surface deformation (1.7 µm) and active flattening (12.3 nmRMS). The mirror produces low-order Zernike modes with a stroke of several tens of micrometer over a correction aperture of 50 mm, which makes the mirror a versatile tool for space telescopes.

Keywords: Active optics, Adaptive optics, Deformable mirror, Vibration damping, Space telescopes, Piezoelectric shunt

1. INTRODUCTION

In recent years, different deformable mirror technologies have been identified, developed and evaluated for aberration correction in space telescopes. These aberrations can stem from gravitational release of ultra-lightweighted mirrors, thermo-elastic deformations or manufacturing processes like residual surface figuring.[1] We refined a deformable mirror which aims at being a versatile tool, not linked to a specific system design. We therefore consider a correction aperture of 50 mm which corresponds to a correction at a pupil plane or a plane conjugated to it. The requirement consolidation is presented in a conference contribution by OHB System.[2]

In this paragraph, we briefly summarize the test results of the previous version of the deformable mirror. The design of the former version of the piezoelectric unimorph mirror and the results of its space qualification have been published[3].[4] In 2015, the former mirror underwent thermal cycling and performance tests in the

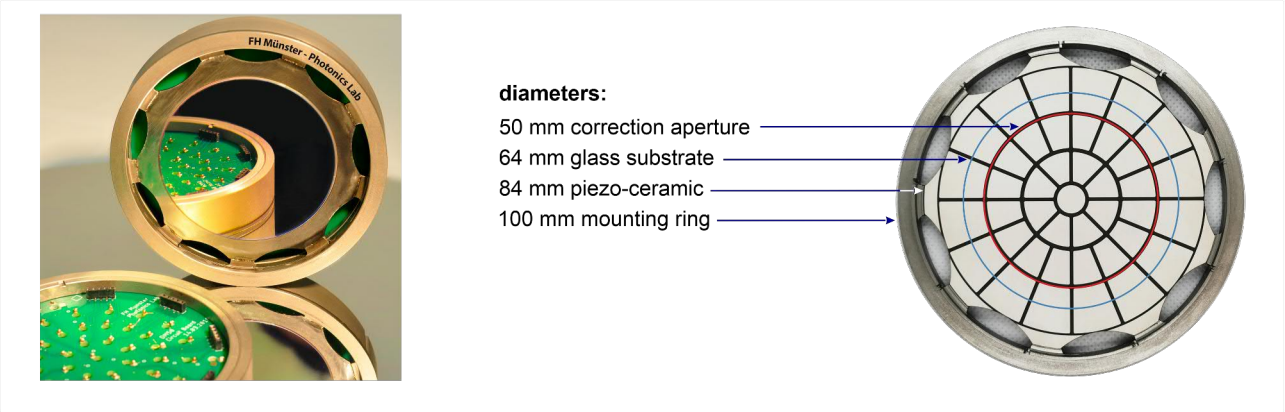

Figure 1. Left: Photo of the isostatic deformable mirror manufactured at Photonics Laboratory. Right: Photo of the structured keystone electrode pattern on the backside of the deformable mirror. The diameters of the 50 mm correction aperture, the 64 mm glass substrate, the 84 mm piezo-ceramic, and the 100 mm mounting ring are indicated.

temperature range between 100 K and 300 K and was exposed to sinusoidal and random vibration, as well as to proton and γ–ray irradiation. The closed loop control bandwidth was 19 Hz and the open loop control bandwidth 100 Hz. The deformable mirror was subjected to laser irradiation with high fluence (5.9 J/cm²), and high average power (1400 W/cm²). No visible degradation of the mirror surface or the mirror performance was observed. Performance verification in thermal vacuum was conducted successfully at temperatures between 100 K and 300 K. The achieved stroke drops with decreasing temperature, as expected for piezoelectric actuators. Thermal cycling between 100 K and 300 K, as well as between −10 °C and 40 °C had no influence on the achieved Zernike amplitudes. The mirror is therefore compatible with the required operational temperature range. In 2015, all functional, operational, and performance requirements were met with the exception of the 18.6 gRMS random vibration. The failure at the high-load vibration test lead to a re-design of the mirror in the framework of an ESA funded GSTP project of Münster University of Applied Sciences and OHB System.

In this follow-up GSTP, titled "Enabling Technologies for Piezo-Based Deformable Mirrors in Active Optics Correction Chains", the focus was put on a consolidation of the requirements and an evolution of the mirror design. Ten deformable mirrors were manufactured in four design variations using four different piezo-electric ceramics. The chosen baseline design is an isostatic unimorph mirror with the soft PZT material PIC151. Topic of this paper is the design evolution and the environmental testing of the new mirror.

2. MIRROR DESIGN AND DEVELOPMENT

Since the actuation principle of unimorph mirrors is based on in-plane forces, they do not rely on rigid support structures and are compact and lightweight. Unimorph mirrors are made from brittle materials like piezo ceramics and glass. The thin mirror structure is prone to oscillations when subjected to dynamic loads. The fracture strength of the piezo ceramic element is reduced by notches along its boundaries that lead to local stress enhancement. Fracture of the piezo element usually occurs due to uncontrolled crack growth, originating at the notches. This results in failure stresses that are much lower than those for metals. We therefore incorporated flexible elements in the monolithic metal ring, to which the piezo-ceramic is mounted. This newly developed *mounting ring* is illustrated in Figure 1. The stress that occurs in a body when its base is forced to follow a certain acceleration depends on the deformation that the body experiences. We could reduce the stress in the piezo ceramic by 90 % by our newly developed isostatic mounting scheme. This scheme transfers most of the deformation under dynamic loads to metal hinge blades. A schematic overview of the mounting design, the hinge blades, and the flexure is illustrated in Figure 2. The flexures have been dimensioned such that their tensile and lateral stiffness are several orders of magnitude higher than their bending stiffness. The bladed flexures define the mirror constraints without introducing bending moments to the brittle piezo-ceramic. The circularly arranged blades minimize bending moments out of the plane of the mirror which results in low global wavefront

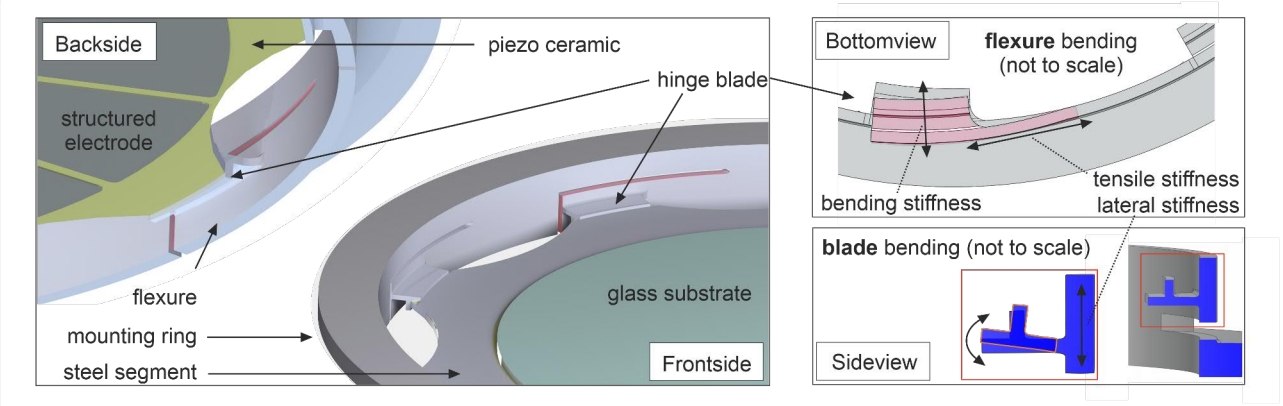

Figure 2. Left: A schematic overview of the mechanical design of the isostatic deformable mirror. The mounting ring features an isostatic design with nine bladed flexures. Right: The bending of the flexure is illustrated (not to scale). The bending stiffness, tensile stiffness as well as the lateral stiffness of the flexure are marked. Additionally, the bending of the blade is pictured (not to scale). The bladed flexures define the mirror constraints without introducing high stress or bending moments to the brittle piezo-ceramic.

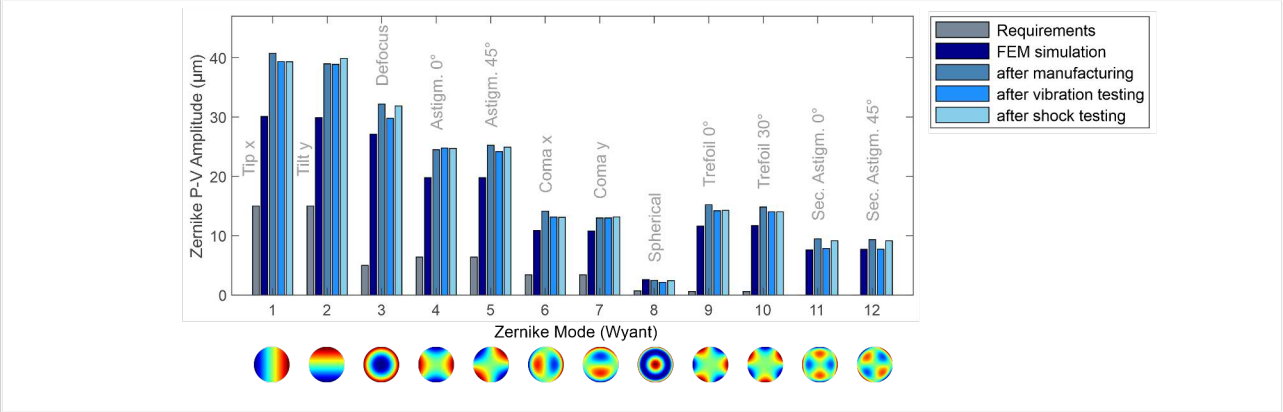

Figure 3. Left: The Zernike amplitudes over the correction aperture of 50 mm after manufacturing, after vibration testing, and after shock testing. No degradation is visible.

error.

In a body with a single degree of freedom, the material stress is reciprocally proportional to the first eigenfrequency squared. By stiffening the mounting, the first eigenfrequency was increased to 570 Hz. In comparison, the deformable mirror in the first project had a first mechanical eigenfrequency of 240 Hz. The challenge was to develop a mounting concept which sustains the launch loads and is capable of coping with residual CTE mismatch but also allows for unhindered actuation of the mirror. The flexures allow the compensation of thermal expansion of the mirror without introducing significant stress into the mirror. Stress would degrade the surface figure of the mirror. Additionally, the mirror assembly has been designed ensuring that the thermal center coincides with the mirrors center of gravity and is exactly located on the optical axis to avoid any unwanted lateral shift under thermal load. The thermal center of a body is defined as the point which experiences no displacement when the body is exposed to temperature change.

The piezoceramic is 700 µm thick and is glued to the mounting ring at the nine hinge blades. We use the piezoelectric material PIC151. The 330 µm thick steel segment (Fe-/Ni alloy Kovar, material number 1.3917) is bonded to the piezoceramic and additionally laser welded to the hinge blades. The 550 µm thick glass substrate (N-BK 10) is bonded to the piezoceramic. The glass substrate is super-polished and has a high-reflectivity dielectric coating to ensure high laser power handling capability which was required by ESA. The adhesives are space qualified and have low out-gassing. The well-matched coefficients of thermal expansion of the mirror's components and the isostatic mounting scheme enable operation over a large temperature range.

The optical characterization of the mirrors includes high resolution interferometric measurements of the unpowered surface deformation as well as measuring the influence functions and active flattening of the deformable mirror. The Zernike amplitudes are illustrated in Figure 3. The Zernike amplitudes are measured after manufacturing, after vibration testing, and after shock testing of the mirror. The project requirements as well as our FEM simulation results are given for comparison. No degradation of the Zernike amplitudes is visible. The amplitudes have been achieved under the condition that the residual RMS surface deviation from the target surface does not exceed $\lambda/14$ (Maréchal-criterion) and that none of the voltages applied to the actuators exceeds the maximum allowed voltage range of $\pm$ 400 V. The voltage restriction is imposed by the driver electronics and not by the piezoelectric material which would allow for higher voltages, the limit depends on the respective material. The unpowered surface deformation was 1.7 µm at best defocus. Active flattening of the mirror surface leads to a peak-to-valley deformation of 95 nm and an RMS deviation of 12.3 nm from a flat surface.

3. RESONANT SHUNTING

The piezoelectric shunt damping technique is based on the electrical to mechanical coupling of piezoelectric materials. The passive shunt circuit dissipates electrical energy that is generated by the piezoelectric element during vibrational excitation. Therefore, the shunt withdraws vibrational energy from the mechanical system and damps the vibration. Passive piezoelectric shunt damping has been a subject of research for the last couple

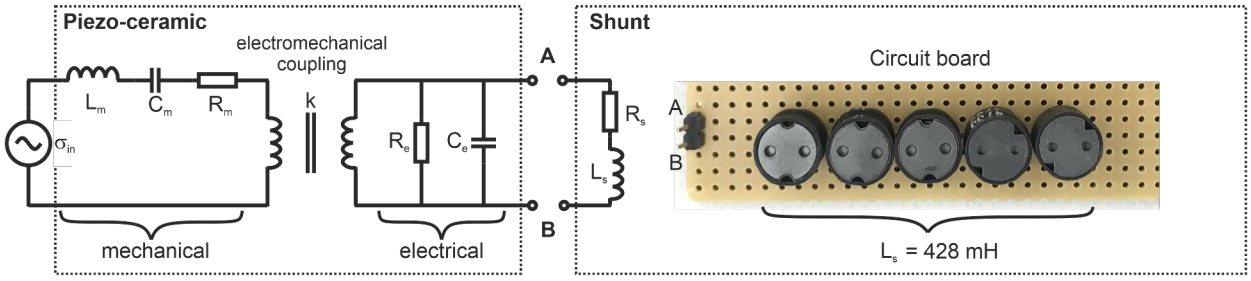

Figure 4. The equivalent circuit diagram of a piezoceramic in the range of a resonance frequency. The mechanical resonance is represented by the RLC-series resonant circuit on the left side. The electro-mechanical coupling is represented by the transformer. The electrical part of the piezoceramic is to be short-circuited with a resonant RL-shunt. The shunt represents a parallel resonant circuit in combination with the electric capacitance of the piezo-ceramic C_e. The circuit is tuned to the mechanical resonant frequency f_R of the piezoceramic. A photo of the used circuit board is given to demonstrate the simplicity of the implementation.

of decades. One benefit of using shunted PZT to damp mechanical systems is that it needs no sensors or advanced control systems. This reduces complexity and minimizes the susceptibility to faults. The equivalent circuit diagram of a piezoceramic and the shunt circuit board are pictured in Figure 4. Single mode and multi-mode vibration suppression can be achieved by designing an external passive shunt circuit. Damping of dominant vibration modes of a flexible structure and their efficiency relies on the precise selection of the shunt components[5] . If the resonance of the passive electrical circuit is equal to that of the mechanical system, the circuit will be in resonance and the vibration energy is dissipated at the resistor in form of heat. Previous studies have already presented the successful application of this technique to suppress vibration modes of unimorph mirrors.[6]

4. VIBRATION TESTING

The vibration test campaign was conducted by applying the "Procedure for Execution of Vibration Tests of Space Equipment (sine and random)", ESA-TECMTV-MSL-PR-006. An electrodynamic combi shaker was used. The mirrors were mounted into an aluminium housing which was mounted onto an aluminium interface plate. This assembly was mounted onto the shaker adapter in two different orientations for vibrations perpendicular and parallel to the mirror surface. The test levels were applied at a rate of 2 octaves per minute for one sweep up and down. Since the sine vibration test was not considered the critical test, we increased the g-levels in one

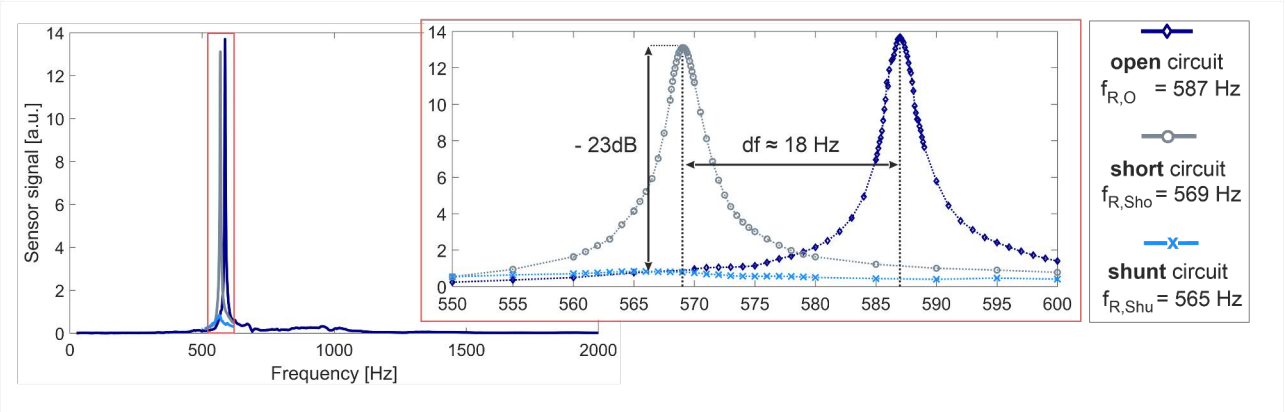

Figure 5. The deformation under acoustic excitation of the mirror. The sine frequencies were computer generated, amplified, and sent to a speaker. The excitation direction is perpendicular to the mirror surface. The resonance frequency of the mirror shifts due to damping. There are three different resonance frequencies: $f_{R,O}$, $f_{R,Sho}$ and $f_{R,Shu}$, which correspond to an open circuit at points A and B in 4, shortening the circuit across A and B, and connecting the shunt circuit board at A and B. The shunt had an inductance of 428 mH and no additional resistor.

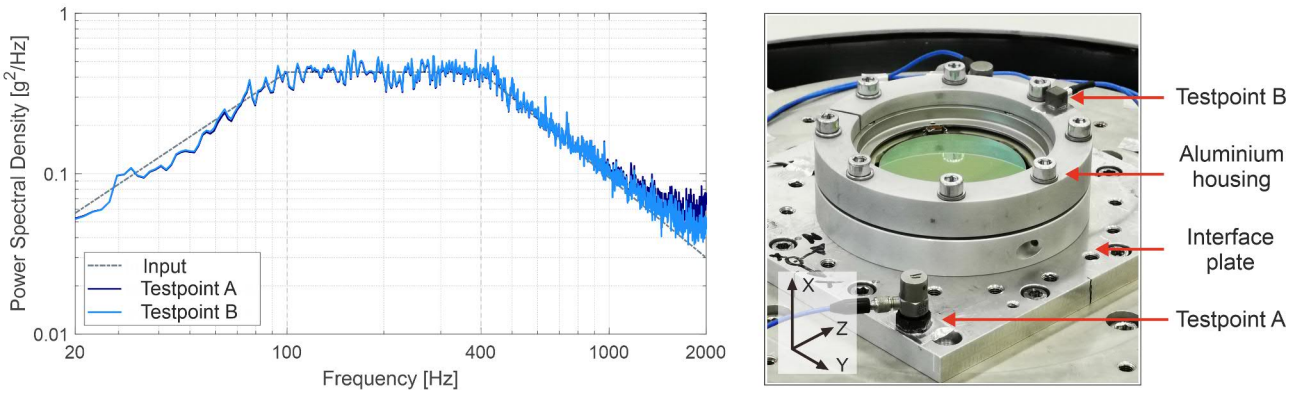

Figure 6. Left: The acceleration spectrum of the random vibration test at 17.8 gRMS. Right: Photo of the deformable mirror in the aluminium housing. The vibration direction is perpendicular to the mirror surface. The two test points are marked. Test point A is tri-axial co-pilot, test point B measures the response of the test adaption (tri-axial miniature accelerometer).

step from −6 dB to the final level of 20 g. The random vibration test level of 17.8 gRMS in the range 20 Hz to 2000 Hz was applied for 2 minutes per axis. For the random vibration test, we increased the test levels in five steps, so that the resulting gRMS levels were −9 dB, −6 dB, −3 dB, −1.5 dB and the final level. The acceleration spectrum of the random vibration test at 17.8 gRMS and the test setup are illustrated in Figure 6. No notching of the acceleration spectra was applied. Vibration tests of the isostatic mirror design were successful for all three tested piezoelectric materials. We tested the soft piezoceramic PIC151 (PI Ceramic) and the hard piezoceramics PIC181(PI Ceramic) and PZ26(Meggitt/Ferroperm).

5. SHOCK TESTING

Shock tests were conducted with a resonant plate setup. The shock level was set to 300 g. The shock tests were conducted with passive electrical shunting as well as without passive electrical shunting. In summary, three qualification level shock tests have been performed for two mirrors of the baseline design achieving the specified shock response spectrum (SRS). The requirement of 50 % of the measured shock spectra above specification was achieved. The general shock boundary test conditions were made in accordance to the ESA Shock Handbook.[7] The shock response spectrum of the tests is pictured in Figure 7.

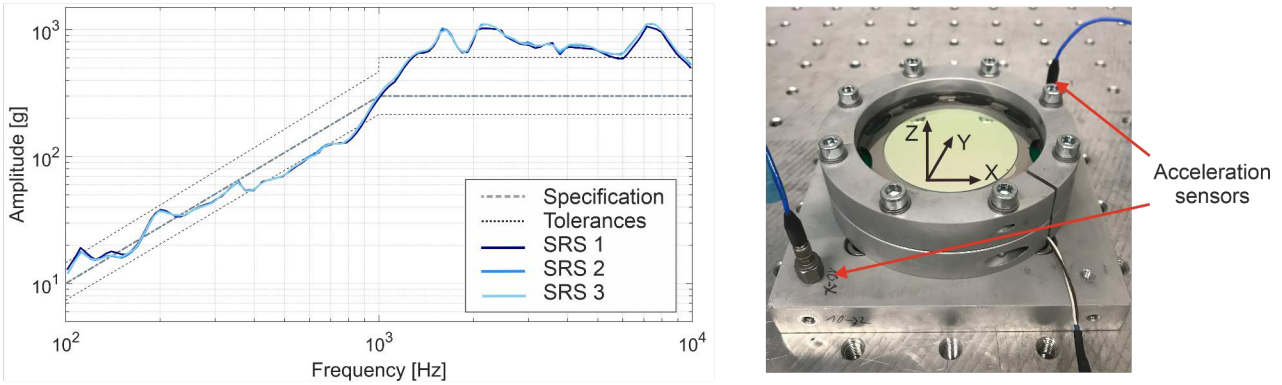

Figure 7. Left: The shock response spectrum of the tests. The deformable mirror was successfully shocked three times with electrical shunting. The specification level as well as the ESA tolerance bands are given. Right: Photo of the test setup. Two accelerations sensors are fastened on the adapter plate.

6. SUMMARY

We have presented the results of the vibration and shock test campaign of a unimorph isostatic deformable mirror. The refined mirror design sustains the launch loads 17.8 gRMS and is capable of coping with residual CTE mismatch while allowing for unhindered actuation of the mirror. Shock tests at 300 gSRS were successful. Taking advantage of the piezoelectric actuation principle, we used a passive inductive shunt to damp the mirrors response to vibration. The deflection of the mirror at the first resonant mode (570 Hz) under acoustic excitation was reduced by −23 dB. The mirror produces low-order Zernike modes with a stroke of several tens of µm over a correction aperture of 50 mm. The newly developed isostatic mounting features flexure blades, which significantly reduce the stress in the piezo-ceramic under dynamic loads. These flexible elements in the monolithic metal ring are reducing the stress in the piezo-ceramic since the deformation under dynamic loads is transferred to the metal hinge blades. FEM simulations yield a stress reduction in the piezo-ceramic by 90 % compared to the previous mirror design of a former GSTP activity. That mirror had been subject to more extensive testing in 2015. Operation in thermal vacuum, exposure to ionizing irradiation, operational life time, and laser power handling capability had been tested. Since the materials as well as the optical coating specifications were not changed, these test results are valid for the refined isostatic design.

Having demonstrated its operability in a relevant environment, we consider the unimorph isostatic deformable mirror matured to a technology readiness level five (TRL) 5. Table 1 summarizes the achieved mirror specifications. Based on the high level of maturity, this mirror is ready for incorporation in future instruments. The achieved TRL of 5 is sufficient for the status of a PDR at payload level and gives a very good basis for future Phase 0 or Phase A/B1 instrument studies.

The achievable Zernike amplitudes can be tailored by modifying the thicknesses of the piezo-ceramic and the glass substrate. Thicker layers result in higher structural rigidity and lower deformations. Thinner layers result in a lower rigidity, making the mirror prone to vibration loads. Larger deformable mirrors with a larger number of actuators can be built using our proven concept. With a prospective correction aperture of 150 mm, the mirror could be used for wide-field or large-aperture space telescopes. The mirror was manufactured with both soft as well as hard piezo-ceramics. Hard piezo-ceramics have several superior characteristics compared to soft piezo materials, such as less creep and hysteresis and a higher E-modulus. The drawback is a reduction of the achievable stroke. We observed a reduction by 60 % between the soft material PIC151 and the hard material PIC181. The isostatic mirrors with the hard piezoceramic material PIC181 and PZ26 also sustained all vibration loads. The possible use of hard piezo-ceramics holds promising advantages for applications with lower optical stroke requirements.

Table 1. Summary of the deformable mirror specifications as well as successful testing.

Optical performance	**Operational performance**
• ± 7.8 mrad Tip/Tilt	• 970 mbar to 1.33×10^{-8} Pa operational atmospheric pressure range
• ± 30 µm Z3 PV-amplitude	• 100 Hz open-loop bandwidth
• ± 25 µm Z4, Z5 PV-amplitude	• 19 Hz closed-loop bandwidth
• ± 7.5 µm Z11, Z12 PV-amplitude	• 570 Hz first mechanical eigenfrequency
• 50 mm correction aperture	• 14 % (soft PZT) / <5 % (hard PZT) hysteresis
• < 2 µm unpowered surface deformation	
• high-reflection dielectric coating	

Structural design	**Thermal performance**
• 61 g quasi-static loads	• 100 K to 333 K operational temperature range
• 20 g sine loads	• 110 K to 353 K non-operational temp. range
• 17.8 gRMS random loads	• 100 K to 300 K thermal cycling
• 300 gSRS shock loads	• proton and γ–ray irradiation
• 41 electrodes in keystone pattern	

ACKNOWLEDGMENTS

Münster University of Applied Sciences and OHB System AG would like to acknowledge the constructive collaboration amongst all parties throughout the project and the support by the European Space Agency under contract number 4000123009/18/NL/PS. We thank ESTEC for the vibration test conduct and KRP Mechatec GmbH for the shock test conduct.

REFERENCES

[1] Hallibert, P., "Enabling technologies for future large optical missions: current perspectives for astronomy and Earth observation at ESA," *Proc. SPIE 10706*, 221–235 (2018).

[2] Maximilian Freudling et al., "Space-qualified piezo based deformable mirror for future instruments with active optics," *International Conference on Space Optics (ICSO)* (2020).

[3] Peter Rausch et al., "Unimorph deformable mirror for space telescopes: environmental testing," *Opt. Expr. 24*, 1528–1542 (2016).

[4] Peter Rausch et al., "Unimorph deformable mirror for space telescopes: design and manufacturing," *Opt. Expr. 23*, 19469–19477 (2015).

[5] O. Thomas, J. Ducarne and J.-F. Deü , "Performance of piezoelectric shunts for vibration reduction," *Smart Materials and Structures* **21**(1) (2012).

[6] D. Alaluf et al., "Damping of piezoelectric space instruments: application to an active optics deformable mirror," *CEAS Space Journal* **6**(11), 543 – 551 (2019).

[7] ESA ESTEC: Requirements & Standards Division, "ECSS-E-HB-32-25A." ECSS, 14 July 2015.